

# Influence of synthesis time on Lanthanum Silicate Apatite ( $\text{La}_{9.33}\text{Si}_6\text{O}_{26}$ ) properties

Noviyanti Atiek Rostika\*, Juliandri, Agustina Shofia Utari and Malik Yoga Trianzar

Department of Chemistry, Faculty of Mathematic and Natural Science, Universitas Padjadjaran, Jl. Raya Bandung-Sumedang KM.

21 Jatinangor, INDONESIA

\*atiek.noviyanti@unpad.ac.id

## Abstract

The crystalline structure of  $\text{La}_{9.33}\text{Si}_6\text{O}_{26}$  apatite-type lanthanum silicates was investigated by X-ray powder diffraction at room temperature. The hydrothermal synthesis condition was optimized to yield ultrafine and highly homogeneous  $\text{La}_{9.33}\text{Si}_6\text{O}_{26}$  powders. The results after rietica refinement indicate that optima crystal apatite structure was formed after being synthesized for six days at 503 K and was in agreement with the  $P63/m$  space group. The lattice parameter of the sample was in agreement with ICSD No 158963.

**Keywords:** Apatite-type lanthanum silicate, ICSD,  $P63/m$  space group, rietica refinement.

## Introduction

Apatite-type lanthanum silicates are rare-earth mineral element crystals with the common formula  $\text{M}_{10}(\text{XO}_4)_6\text{O}_2$  where M is a metal such as rare-earth or alkaline and X is a p-block element such as phosphorus (P), silicate (Si) or germanium (Ge)<sup>1</sup>. Apatite-type lanthanum silicates with high oxide ion conductivity offer the potential advantage as electrolytes in Solid Oxide Fuel Cell<sup>2,3</sup>. This is possible because the structure of the apatite has the oxygen ions in the channel conduction (c-axis)<sup>4</sup>. The crystal structure of the apatite is shown in fig. 1.

Apatite oxide was successfully synthesized through various methods including solid state reaction<sup>5</sup>, hydrothermal<sup>6</sup> and sol-gel<sup>7</sup>. Hydrothermal is among the simple methods that can be applied for the synthesis of apatite-type lanthanum silicate, due to its low operation temperature and easy preparation. In addition, the resulted product has high purity and crystallinity<sup>6,8</sup>. Ferdov prepared apatite at 230°C for seven days<sup>7</sup> from  $\text{LaCl}_3 \cdot 7\text{H}_2\text{O}$  and  $\text{SiO}_2$ ; the product has a nano-size apatite. Meanwhile Noviyanti et al<sup>6</sup> carried out the same experiment at 240°C for three days from  $\text{La}_2\text{O}_3$  and  $\text{Na}_2\text{SiO}_3$  and obtained apatite with a micro-size. This suggests that different reaction time, temperature and precursor of synthesis directly affect the properties and characters of apatite crystal.

This research aims to investigate the effect of reaction time (1-6 days) of synthesis on the structure, size and crystallinity of apatite lanthanum silicate.

## Material and Methods

**Synthesis of apatite:**  $\text{La}_2\text{O}_3$  powder ( $\text{La}_2\text{O}_3$  99.999%; Sigma Aldrich) was calcinated at 1100°C for 10 h.  $\text{Na}_2\text{SiO}_3$

( $\text{Na}_2\text{SiO}_3$  97%; Sigma Aldrich) was diluted in 50 mL of 3 M of NaOH (NaOH 99%; Merck). The reactants in the correct stoichiometric ratio were thoroughly mixed and hydrothermally synthesized at 503 K for six different durations namely 1-6 days. The resulted apatite was washed with demineralizer water and then heated at 393 K for 24 h to remove the water.

**Structure determination:** Phase purity was determined by X-ray diffraction (Philips Analytical, PW1710) using Cu-K $\alpha$  ( $\lambda = 1.5406 \text{ \AA}$ ) at room temperature. The diffraction pattern obtained was then compared to the pattern diffraction standards data obtained from the inorganic crystal structure data (ICSD).

Crystal system and lattice parameters were obtained by refining the X-ray diffraction pattern using the Le Bail method with RIETICA software. The Le Bail method compares the lattice parameters of standards from ICSD to the lattice parameters of the material. The particle size was determined by particle size analyzer (PSA Beckman Coulter type LS 13 320).

## Results and Discussion

Fig. 2 illustrates the XRD diffraction pattern of apatite at various synthesis times, at 513 K, after being washed with distilled water and heated to 393 K.

Overall, the typical peaks of lanthanum silicate at  $2\theta$  of 21.1°; 22°; 24.8°; 27°; 28°; 30.7°; 30.9°; 31.9°; 32.7°; 38.5°; 39°; 40.7°; 42°; 42.9°; 45°; 45°; 46.3°; 47.4°; 48.8°; 49.6° appear in all diffractograms. This indicates that lanthanum silicate apatite was successfully obtained at 513 K. The diffraction pattern is in line with the diffraction pattern  $\text{La}_{9.33}\text{Si}_6\text{O}_{26}$  (ICSD No. 158963) and in agreement with previous works in the literature<sup>10-12</sup>. Small impurities (estimated secondary phase is  $\text{La}_2\text{SiO}_5$ ) were detected marked by a peak at  $2\theta$  of 21.1°. The impurities peak at 1-3 days synthesis was higher than that at 4-6 days.

In order to ensure the best fit structure, we attempt to refine the structure by using the Le Bail method from Rietica, fit with the three possible space groups of apatite, namely,  $P_{-3}$ ,  $P_{63}$  and  $P_{63/m}$ . Le bail refinement shows that (Table 1) the apatite prepared by hydrothermal synthesis has a hexagonal structure with a space group  $P_{63/m}$ .

The lattice parameter of apatite obtained from six days synthesis (Table 1) is similar to the value of the lattice parameter of apatite of  $\text{La}_{9.33}\text{Si}_6\text{O}_{26}$  resulting from the sol-

gel method, i.e.  $a = b = 9.726(3) \text{ \AA}$  and  $c = 7.184(5) \text{ \AA}$ <sup>13</sup>; and solid-state reaction i.e.  $a = b = 9.721(3) \text{ \AA}$  and  $c = 7.187(3) \text{ \AA}$ <sup>14</sup>.

Due to the detection of small impurities, it is worthy to determine certain levels of secondary phase. We prepared refinement using two phases ( $\text{La}_{9,33}\text{Si}_6\text{O}_{26}$  and  $\text{La}_2\text{SiO}_5$ ) on all of the samples. The percentage of secondary phase of apatite,  $\text{La}_2\text{SiO}_5$ , is listed in Table 2. The lowest level of impurities was obtained from the sample prepared for six days, which is in agreement with the lowest intensity of peak at  $2\theta 15^\circ$ .

As mentioned previously, there are three types ( $P_{-3}$ ,  $P_{63}$ ,  $P_{63/m}$ ) of space groups for  $\text{La}_{9,33}\text{Si}_6\text{O}_{26}$ . All the samples were refined using possible space group reliability weight profile

of our material, which has the lowest reliability profile and reliability weight profile on the  $P_{63/m}$  space group (Table 3). The longer is the synthesis time, the longer is the reaction time between the precursors to form the  $\text{La}_{9,33}\text{Si}_6\text{O}_{26}$  apatite, so that the rearrangement time is also increased. The speed of the rearrangement increases with the increase in the synthesis time, so that the resulting particle size becomes smaller.

Based on fig. 3, there are changes in particle size distribution that occur at different reaction times of apatite synthesis. The longer is reaction time, the smaller is size of apatite's particle. From Table 4, as expected the homogeneity of the particle size increased, together with the longer reaction time of synthesis. However, the sixth day resulted in lower homogeneity which suggests that a longer reaction time is needed for better homogeneity.

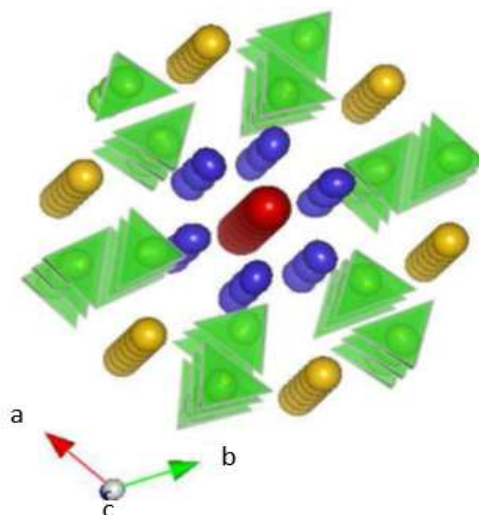


Fig. 1: C-axis view of the crystal structure of  $\text{La}_{9,33}\text{Si}_6\text{O}_{26}$  showing the  $\text{SiO}_4$  group as tetrahedral and La  $4f$  site (brown spheres), La  $6h$  site (blue spheres) and O  $2a$  site (red spheres) in the conduction channel.

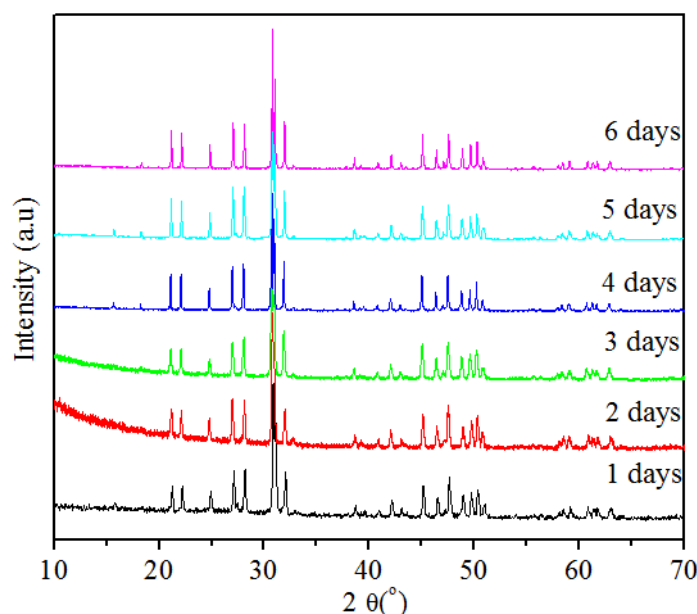


Fig. 2: XRD diffraction patterns of apatite  $\text{La}_{9,33}\text{Si}_6\text{O}_{26}$  at different time of synthesis (1-6 days).

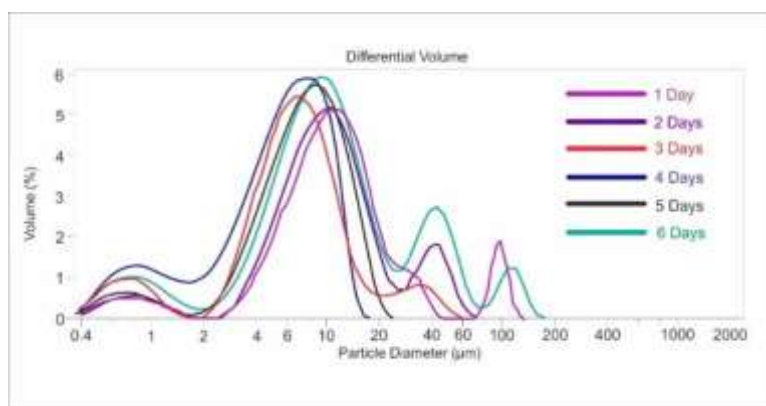


Fig. 3: Distribution of Particle size of  $\text{La}_{9.33}\text{Si}_6\text{O}_{26}$  samples at (a) 1 day (b) 2 days (c) 3 days (d) 4 days (e) 5 days and (f) 6 days.

Table 1  
 Lattice parameter of apatite  $\text{La}_{9.33}\text{Si}_6\text{O}_{26}$  prepared at various reaction time.

Reaction time (day)	$a=b$ (Å)	$C$ (Å)	Cell volume	$R_p$	$R_{wp}$
1	9.817(1)	7.256(1)	605.651	7.14	9.57
2	9.751(1)	7.230(1)	595.292	7.14	9.62
3	9.718(1)	7.180(1)	587.223	6.28	8.23
4	9.822(1)	7.259(1)	606.465	8.78	12.65
5	9.732(1)	7.193(1)	589.962	7.40	11.01
6	9.722(1)	7.186(1)	588.219	7.93	11.15

Table 2  
 Percentage of secondary phase of apatite  $\text{La}_{9.33}\text{Si}_6\text{O}_{26}$

Sample	Synthesis Time (day)	Secondary Phase, $\text{La}_2\text{SiO}_5$ (%)
$\text{La}_{9.33}\text{Si}_6\text{O}_{26}$	1	85.7
	2	32.3
	3	26.9
	4	38.9
	5	48.9
	6	25.1

Table 3  
 Comparison of  $\text{La}_{9.33}\text{Si}_6\text{O}_{26}$  lattice parameter at various space group

Space Group	$a=b$ (Å)	$C$ (Å)	$R_p$	$R_{wp}$
$P 63$	9.672	7.150	8.86	12.00
$P -3$	9.759	7.214	8.25	11.44
$P 63/m$	9.722	7.186	7.93	11.15

Table 4  
 Particle size of apatite type lanthanum silicate  $\text{La}_{9.33}\text{Si}_6\text{O}_{26}$

Sample	Reaction time(day)	The distribution of particle size		Comparison Mean: median (µm)
		Mean (µm)	Median (µm)	
$\text{La}_{9.33}\text{Si}_6\text{O}_{26}$	1	17.62	10.78	1.635
	2	12.95	9.526	1.359
	3	8.44	6.502	1.299
	4	4.734	4.183	1.132
	5	8.126	7.704	1.055
	6	18.50	9.729	1.902

## Conclusion

Apatite-type of  $\text{La}_{9.33}\text{Si}_6\text{O}_{26}$  was successfully synthesized using the hydrothermal method at 513 K for various durations (1-6 days). The refinement resulted in the sixth day sample being the most valuable due to its lattice parameter value which is similar to ICSD standard and its lower percentage of secondary phase. Among three space groups of apatite,  $P_{63/M}$  was the best space group because it has lower  $R_p$  and  $R_{wp}$  values. According to particle size distribution, the fifth day had the smallest and highest homogeneity.

## Acknowledgement

We would like to thank the DIKTI (RDUPT No. 718/UN6.3.1/PL/2017) for funding this research.

## References

1. Nakayama S., Aono H. and Sadaoka Y., Ionic Conductivity of  $\text{Ln}_{10}(\text{SiO}_4)_6\text{O}_3$  (Ln = La, Nd, Sm, Gd and Dy), *Chemistry Letters*, **24**, 431-435 (1995)
2. Kendrick E., Islam M.S. and Slater P.R., Developing apatites for solid oxide fuel cells: insight into structural, transport and doping properties, *Journal of Material Chemistry*, **17**, 3104-3111 (2007)
3. Sansom J.E.H., Najib A. and Slater P.R., Oxide ion conductivity in mixed Si/Ge-based apatite-type systems, *Solid State Ionics*, **175(1-4)**, 353-355 (2004)
4. Panteix P.J., Julien I., Bernache-Assollant D. and Abelard P., Synthesis and characterization of oxide ions conductors with the apatite structure for intermediate temperature SOFC, *Materials Chemistry and Physics*, **95(2-3)**, 313-320 (2006)
5. Cao X.G. and Jiang S.P., Synthesis and characterization of lanthanum silicate oxyapatites co-doped with A (A  $\frac{1}{4}$  Ba, Sr and Ca) and Fe for solid oxide fuel cells, *Journal of Materials Chemistry A*, **2**, 20739-20747 (2014)
6. Noviyanti A.R., Ismunandar, Prijamboedi B. and Marsih I.N., Hydrothermal Preparation of Apatite-Type Phases  $\text{La}_{9.33}\text{Si}_6\text{O}_{26}$  and  $\text{La}_9\text{M}_1\text{Si}_6\text{O}_{26.5}$  (M = Ca, Sr, Ba), *ITB Journal of Science*, **44(2)**, 193-203 (2012)
7. Tao S.W. and Irvine J.T.S., Preparation and characterisation of apatite-type lanthanum silicates by a sol-gel process, *Materials Research Bulletin*, **36(7-8)**, 1245-1258 (2001)
8. Ferdov S., Ferreira R.A.S. and Lin Z., Hydrothermal Synthesis, Structural Investigation, Photoluminescence Features and Emission Quantum Yield of Eu and Eu-Gd Silicates with Apatite-Type Structure, *Chemistry of Materials*, **18**, 5958-5964 (2006)
9. Ferdov S., Rauwel P., Lin Z., Ferreira R.A.S. and Lopes A., A simple and general route for the preparation of pure and high crystalline nanosized lanthanide silicates with the structure of apatite at low temperature, *Journal of Solid State Chemistry*, **183(11)**, 2726-2730 (2010)
10. Nakayama S., Kageyama T., Aono H. and Sadaoka Y., Ionic Conductivity of Lanthanoid Silicates,  $\text{Ln}_{10}(\text{SiO}_4)_6\text{O}_3$  (Ln = La, Nd, Sm, Gd, Dy, Y, Ho, Er and Yb), *Journal of Materials Chemistry*, **5**, 1801-1805 (1995)
11. Nakayama S., Sakamoto M., Higuchi M., Kodaira K., Sato M., Kakita S., Suzuki T. and Itoh K., Oxide ionic conductivity of apatite type  $\text{Nd}_{9.33}(\text{SiO}_4)_6\text{O}_2$  single crystal, *Journal of the European Ceramic Society*, **19(4)**, 507-510 (1999)
12. Vincent A., Savignat S.B. and Gervais F., Elaboration and ionic conduction of apatite-type lanthanum silicates doped with Ba,  $\text{La}_{10-x}\text{Ba}_x(\text{SiO}_4)_6\text{O}_{3-x/2}$  with  $x = 0.25-2$ , *Journal of the European Ceramic Society*, **27**, 1187-1192 (2007)
13. Célérier S., Laberty C., Ansart F., Lenormand P. and Stevens P., New chemical route based on sol-gel process for the synthesis of oxyapatite  $\text{La}_{9.33}\text{Si}_6\text{O}_{26}$ , *Ceramics International*, **32(3)**, 271-276 (2006)
14. Sansom J.E.H., Kendrick E., Tolchard J.R., Islam M.S. and Slater P.R., A comparison of the effect of rare earth vs Si site doping on the conductivities of apatite-type rare earth silicates, *Journal of Solid State Electrochemistry*, **10(8)**, 562-568 (2006).